

The Second Stars

Falk Herwig

Los Alamos National Laboratory

Los Alamos, Theoretical Astrophysics Group, NM 87544, USA

fherwig@lanl.gov

Abstract

The ejecta of the first probably very massive stars polluted the Big Bang primordial element mix with the first heavier elements. The resulting ultra metal-poor abundance distribution provided the initial conditions for the second stars of a wide range of initial masses reaching down to intermediate and low masses. The importance of these second stars for understanding the origin of the elements in the early universe are manifold. While the massive first stars have long vanished the second stars are still around and currently observed. They are the carriers of the information about the first stars, but they are also capable of nuclear production themselves. For example, in order to use ultra or extremely metal-poor stars as a probe for the r-process in the early universe a reliable model of the s-process in the second stars is needed. Eventually, the second stars may provide us with important clues on questions ranging from structure formation to how the stars actually make the elements, not only in the early but also in the present universe. In particular the C-rich extremely metal-poor stars, most of which show the s-process signature, are thought to be associated with chemical yields from the evolved giant phase of intermediate mass stars. Models of such AGB stars at extremely low metallicity now exist, and comparison with observation show important discrepancies, for example with regard to the synthesis of nitrogen. This may hint at burning and mixing aspects of extremely metal-poor evolved stars that are not yet included in the standard picture of evolution, as for example the hydrogen-ingestion flash. The second stars of intermediate mass may have also played an important role in the formation of heavy elements that form through slow neutron capture reaction chains (s-process). Comparison of models with observations reveal which aspects of the physics input and assumptions need to be improved. The s-process is a particularly useful diagnostic tool for probing the physical processes that are responsible for the creation of elements in stars, like for example rotation. As new observational techniques and strategies continue to penetrate the field, for example the multi-object spectroscopy, or the future spectroscopic surveys, the extremely metal-poor stars will play an increasingly important role to address some of the most fundamental and challenging, current questions of astronomy.

1 Introduction

One of the most intriguing questions of astrophysics and astronomy is the origin of the elements in the early universe, and how this relates to the first formation of structure. About 200,000 years after the Big Bang the epoch of structure formation emerged and the first stars were born from the initial, pristine baryonic matter. Without any elements heavier than helium to provide cooling, the first stars that formed from the baryonic matter trapped in the emerging mini-dark matter halos were probably very massive, greater than $30 M_{\odot}$ (e.g. Abel et al., 2002). These massive stars burned through their available fuel in about one to two million years, exploded as supernovae, and dispersed the first elements heavier than helium into the nascent universe, or collapsed into black holes. These first events of stellar evolution influenced their early universe neighborhood, and determined under which conditions and with which initial abundance low-mass stars with masses like the Sun eventually formed. These take about 100 to 1000 times longer to form than more massive stars. Thus, by the time the first low-mass stars formed there was already a small amount of heavier elements present. Such low-mass stars are really the second stars, stars which formed from a non-primordial abundance distribution. These second stars are important because while the massive first stars have long since vanished, some second stars are still around. Their importance lies in their capacity as carriers of the information about the formation and evolution of those long gone first generations of stars. The second stars are also important because of the nuclear production they are capable of by themselves (for example the first s-process in the second stars). Observations of such second stars are now emerging in increasing quantity and with high-resolution spectroscopic abundance determination (Beers & Christlieb, 2005).

There are a number of strategies to find ultra and extremely metal-poor stars. The most effective appears to be spectroscopic surveys. Most of the EMP and UMP stars have been discovered in the HK survey (Beers et al., 1992) and the Hamburg/ESO survey (HES Christlieb et al., 2001). Here, I designate somewhat arbitrarily ultra metal-poor (UMP) stars as those with $[Fe/H] \leq -3.5$ ($Z \leq 6 \cdot 10^{-6}$) and extremely metal-poor (EMP) stars as those with $[Fe/H] \leq -1.8$ ($Z \leq 3 \cdot 10^{-4}$). EMP stars include the most metal-poor globular clusters. UMP stars are rare and hard to find in the spectroscopic surveys. Only approximately a dozen have been reported so far, with the present record holder HE 0107-5240 at $[Fe/H] = -5.4$ (Christlieb et al., 2002; Christlieb et al., 2004). At and below this metallicity spectral features are so weak that even the 10m class telescopes are barely suitable for the job.

The formation mode of the second stars depends on a complex history of events, each of which may leave signatures in the observed abundances of EMP and in particular the UMP stars. These events include the ionizing radiation of the very first primordial stars and the expansion of the associated H II regions, their effect on possibly primordial star formation in neighboring mini-dark matter halos, as well as possibly the metal enrichment from a pair-

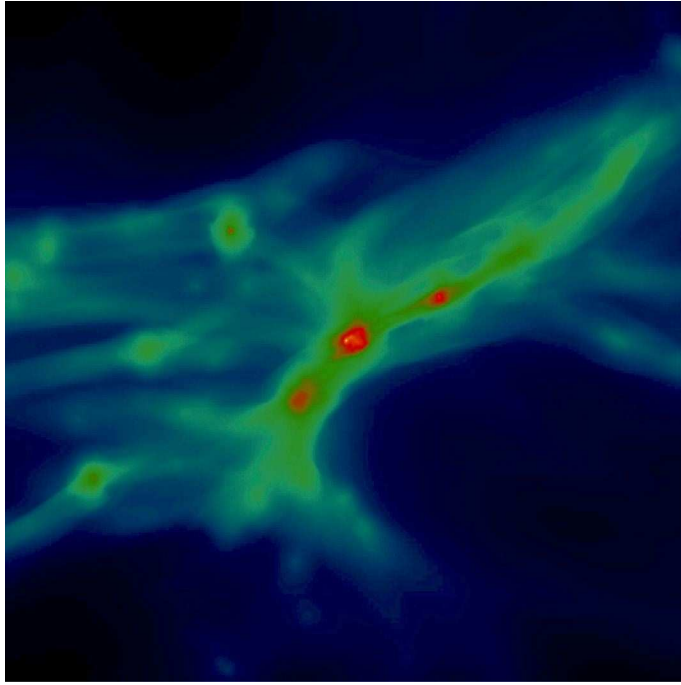


Figure 1: Distribution of baryonic matter clustering around a cosmological dark matter halo in a hydrodynamics and N-body simulation at redshift $z \approx 17$ (O’Shea et al., 2005). The projection volume of 1.5 proper kiloparsecs on a side is centered on the halo where the first population III star in this region will form. This halo is surrounded by other halos in which the second generations of primordial and/or metal-enriched stars will form. Star formation in these neighboring halos is effected by the ionizing radiation from the first star formation in the center halo, and may include primordial or ultra metal-poor intermediate mass stars.

instability supernova, depending on the mass of the first primordial stars. These processes and the cosmological assumption that fix the underlying dark-matter structure will eventually determine the abundance distribution of the EMP and UMP stars now discovered and analyzed. The most recent studies confirm that the very first primordial stars are massive (O’Shea et al., 2005). However in these calculations the effect of the ionization from star formation in nearby mini-dark matter halos is taken into account, and it is found that the following generation of primordial stars may include intermediate mass stars.

The most metal-poor stars are potentially an extremely powerful tool to study star formation and evolution in the early universe (Beers & Christlieb, 2005). These stars with metallicities reaching in excess of 5 orders of magnitude in metallicity below the solar metallicity often show abundance distri-

butions that are very different from the solar abundance distribution. The solar abundance distribution is the result of a long galactic chemical evolution, reflecting the cumulative result of mixing and nuclear processing of many generations of stars of a wide range of masses. The most metal-poor stars are very old and have formed very early, at the onset of galactic chemical evolution. It is therefore reasonable to assume that the abundance pattern in these second stars are the result of only few different sources and corresponding stellar nuclear production sites. The goal is to identify these nuclear production sites and the mechanisms and processes through which the corresponding stellar ejecta have been brought together in the star formation cloud of the second stars. An important part of the problem is to account for self-pollution or external pollution events that may have altered the stellar abundances between the time of second star formation and observation.

As the number of EMP and UMP stars with detailed abundance continuously grows one can discern certain abundance patterns. A very unusual sub-group are the carbon-rich EMP and UMP stars. Observations indicate that many of these stars are polluted by Asymptotic Giant Branch (AGB) binary companions. This implies that reliable models of AGB stars including their heavy element production through the s-process at extremely low metallicity are required to understand these stars, and to disentangle the AGB contribution from other sources that have contributed to the observed abundance patterns. In the following section the carbon-rich EMP and UMP stars will be discussed in more detail. In § 3 current models of EMP intermediate mass stars and their uncertainties are presented. Such models have important applications for the emerging field of near-field cosmology, which uses galactic and extra-galactic stellar abundances to reconstruct the processes that lead to the formation of our and other galaxies (§ 4). Then, ongoing work – both observational and theoretical – to determine the nucleosynthesis of nitrogen at extremely low metallicity is described (§ 5) and § 6 covers the hydrogen-ingestion flash in born-again giants, because this type of events may be important for EMP AGB stars as well, and may indeed be a major source of nitrogen in these stars. § 7 deals with the *s* process, and how it can be used as a diagnostic tool to improve the physics understanding of stellar mixing. Finally, and before some forward looking concluding remarks (§ 9) the importance of nuclear physics input for the question of C-star formation will be discussed in § 8.

2 The C-rich most metal-poor stars

About 20...30% of all EMP and UMP stars show conspicuous enrichment of the CNO elements, most notably C. For example, CS 29497-030 (Sivarani et al., 2004) has $[\text{Fe}/\text{H}] = -2.9$, $[\text{C}/\text{Fe}] = 2.4$, $[\text{N}/\text{Fe}] = 1.9$, $[\text{O}/\text{Fe}] = 1.7$, and $[\text{Na}/\text{Fe}] = 0.5$. Others, like LP 625-44 ($[\text{Fe}/\text{H}] = -2.7$ Aoki et al., 2002) or CS 22942-019 ($[\text{Fe}/\text{H}] = -2.7$ Preston & Sneden, 2001), have a similar overabundance of C, but smaller N ($[\text{N}/\text{Fe}] = 1.0$ for LP 625-44) and larger Na

($[\text{Na}/\text{Fe}] = 1.8$ for LP 625-44). Many of the heavier elements, like Ti, Cr, Mn or Zn in CS 29497-030 are either not overabundant or rather somewhat underabundant compared to the solar distribution.

Large overabundances of N and Na are not predicted by standard models of massive stars, neither for Pop III (Heger & Woosley, 2002) nor at larger metallicity (Woosley & Weaver, 1995). Primary production of N requires to expose the He-burning product C to H-burning again. Such a condition is encountered in massive AGB stars during hot-bottom burning (Herwig, 2005). Na is made in C-burning in massive stars but its final abundance is sensitive to the neutron excess, and thus scales less than linear with metallicity. If primary ^{14}N is exposed to He-burning it will lead to the production of ^{22}Ne . Either an additional proton collected in hot-bottom burning, or a neutron from the $^{22}\text{Ne}(\alpha, n)^{25}\text{Mg}$ reaction in the He-shell flash of AGB stars can then lead to primary ^{23}Na production. This process leads to significant Na overabundances in standard AGB stellar models of very low or zero metallicity (Herwig, 2004b; Siess et al., 2004).

The overabundances of C, N and Na are not the only indication that the abundances in C-rich EMP stars are at least partly caused by AGB stellar evolution. All of the objects mentioned above, and in fact most C-rich EMP stars show in some cases significant overabundances of the s-process elements. In addition they reveal their binarity through radial velocity variations, corresponding to binary periods of a few days in the case of HE 0024-2523 (Lucatello et al., 2003) to more typically one to a dozen years. In fact, in their statistical analysis Lucatello et al. (2004) find that observations of radial velocities of CEMP-s stars (C-rich EMP stars with s-process signature) obtained to date is consistent with a 100% binarity rate of CEMP-s stars.

HE 0107-5420 is currently the intrinsically most metal-poor star with $[\text{Fe}/\text{H}] = -5.3$. However, the total metal abundance in terms of elements heavier than He is quite large. In particular the CNO elements are significantly overabundant compared to the solar abundance ratios, with $[\text{C}/\text{Fe}] = +4.0$, $[\text{N}/\text{Fe}] = +2.4$ (Christlieb et al., 2004), and $[\text{O}/\text{Fe}] = +2.3$ (Bessell et al., 2004). The large overabundance alone indicate that only a few nuclear sources were involved in creating this abundance pattern. Together with the low Fe abundance the large CNO abundances require a primary production of the CNO elements. A primary nucleosynthesis production chain in a star is based only on the primordial elements H and He. A secondary production in contrast requires heavier elements already to be present in the initial element mix at the time of star formation. For example, standard models of massive stars predict a secondary production of N from CNO cycling of C and O that is initially present from earlier generations of stars.

HE 0107-5420 is a good example to discuss the possible nuclear production sites that may be important at the lowest metallicities. Certainly the production of the first massive Pop III stars plays an important role. Umeda & Nomoto (2003) have discussed the observed abundance pattern within the framework of mixing and fallback of the ejecta during the explosion of supernovae that eventually form a black hole. They show that

the mixing and fallback parameters can be chosen in a way that accounts for much of the observed pattern. For example, their model correctly reflects the large observed Fe/Ni ratio, and the large C/Fe and C/Mg ratios. The model does predict a significant N overabundance but it quantitatively falls short of matching the observed value. Their model predicts the characteristic odd-even effect that reflects the small (or missing) neutron-excess of the primordial nuclear fuel. One of the observed species that hints that HE 0107-5420 may not have such a pronounced odd-even pattern is Na. The observed overabundance is $[Na/Fe] = 0.8$, more than 1.5 dex above the model prediction from the mixing and fallback supernova. Unfortunately, for the heavy trans-iron elements only upper limits could be derived so far, which prohibits definite access to the s- and r-process abundances in HE 0107-5420. At this point Na and to a lesser extent N are the major indicators that some additional sources are part of the nuclear production site inventory that caused the abundance pattern in this most metal-poor star.

Without better guidance from ab-initio coupled structure and star formation simulations – such as shown in Fig. 1 – several scenarios have to be considered. Material from the first supernova could be ejected from the corresponding halo and injected into a neighbouring halo. This metal enrichment could lead to the formation of an intermediate mass star, for example a very massive AGB star, maybe even a super-AGB star that eventually ends in a ONeMg core-collapse supernova. As shown in § 3 a contribution from such stars can account for both Na as well as N, but more detailed models of this particular scenario need to be done for quantitative comparison. A low-mass star like HE 0107-5420 could then form from the combined nuclear production of these two sources, a roughly $25 M_{\odot}$ black hole forming supernova and a massive AGB or super-AGB star.

Alternatively the low-mass star forms from the ejecta of just one supernova, and this initial abundance pattern is modified by self-pollution. HE 0107-5420 is in fact a giant on the first ascent. Observations, in particular of globular cluster red giants show that mixing and nuclear processing of C into N below the deep convective envelope lead to secondary N production (Denissenkov & Vandenberg, 2003; Weiss et al., 2004). This could explain the quantitative discrepancy between the observed N abundance and the model by Umeda & Nomoto (2003). However, the rather large carbon isotopic ratio $^{12}C/^{13}C \sim 60$ implies that self-pollution can not account for the observed Na abundance, in particular assuming the absence of ^{22}Ne which is a secondary nucleosynthesis product in massive stars.

This leads to the external pollution scenario that is frequently considered in this context. As mentioned above many CEMP stars are in fact in binary systems, and the abundance signatures seen in these C-rich very metal-poor stars could be – in part – the result of mass transfer from the AGB progenitor of a white dwarf companion. For HE 0107-5420 Suda et al. (2004) discuss this possibility in detail. For the evolution of primordial AGB stars they consider the possibility of the H-ingestion flash, a process in which the He-shell flash convection zone reaches outward into the H-rich envelope, resulting

in a peculiar nucleosynthesis and mixing regime. Such events are known at solar metallicity to cause a significant fraction of young white dwarfs to evolve for a short period of time back to the AGB (born-again evolution, § 6), and the most prominent representative of this class of objects is Sakurai's object (Duerbeck et al., 2000).

3 Stellar evolution models for the second stars

As discussed in the previous section the evolution of low- and intermediate mass stars at zero or extremely or ultra metal-poor abundance is essential for studying the most metal-poor stars and their cosmological origin and environment. This section deals first with the evolution of AGB stars that may have formed from Big Bang material. A possibly important evolutionary phase - the H-ingestion flash triggered by the He-shell flash - has been observed in models of Pop III and even in models of non-zero but ultra-low metal content (§ 3.2). Finally the evolution and yields of extremely metal-poor TP-AGB stars is described. The evolution of Pop III massive stars is discussed, for example, by Heger & Woosley (2002).

3.1 Pop III AGB evolution

Simulations show that many of the overall properties of Pop III intermediate mass stellar models (Chieffi et al., 2001; Siess et al., 2002) probably apply to ultra metal-poor stars as well. At $Z = 0$ the initial thermal pulses may show peculiar convective mixing events at the core-envelope boundary during or after the actual He-shell flash. But eventually the models enter a phase of rather normal thermal pulse AGB evolution, with regular thermal pulse cycles, third dredge-up, hot-bottom burning and mass loss. Many uncertainties of the Pop III stellar evolution is related to the possibility of flash-burning that is not yet well understood (§ 3.2).

$Z = 0$ stellar evolution is different from evolution at higher metal content because CNO catalytic material for H-burning is initially absent. Burning hydrogen via the pp-chain requires a higher temperature than H-burning via the CNO cycle. Eventually the triple- α process will provide some C, and a mass fraction as low as 10^{-10} is sufficient to switch H-core burning to CNO cycling. During He-core burning some C is produced outside the convective core and a tail of carbon reaches from the convective core out toward the H-shell. After the end of He-core burning, and depending on the initial mass, this carbon and some nitrogen is mixed into the envelope. According to Chieffi et al. (2001) this second dredge-up raises the envelope C-abundance above $10^{-7} M_{\odot}$ for $M_{ini} > 6 M_{\odot}$. For such a C-abundance the H-shell is fully supported by CNO cycling. As a result the thermal pulse AGB evolution is like that of the ultra metal-poor cases.

Models with initial masses below $6 M_{\odot}$ show a peculiarity that is unknown in more metal-rich models. After an initial series of weak thermal pulses the

H-shell forms a convection zone when it re-ignites after the He-shell flash (Chieffi et al., 2001; Siess et al., 2002; Herwig, 2003). The lower boundary of this convection zone is highly unstable, because it coincides with the opacity discontinuity that marks the core-envelope interface. Even small amounts of mixing will drive flash-like burning and deep mixing, as protons enter a ^{12}C -rich zone. It seems that the details of the evolution of the H-shell convection zone is not important as this one-time event leads to deep dredge-up and enrichment of the envelope with a sufficient amount to support regular CNO cycle burning in the H-shell thereafter. Accordingly, these lower-mass cases will evolve like extremely metal-poor stars too, and the $Z = 0$ models discussed here can be used as proxies for what is in reality born as an ultra metal-poor star.

The effect of rotationally induced mixing processes may alter the evolution of low- and intermediate-mass stars and very low metallicity even before the AGB and lead to a qualitatively different thermal pulse evolution. Meynet & Maeder (2002) describe models for metallicity $Z = 10^{-5}$ in which ^{12}C and ^{16}O is mixed out of the He-burning core and up to the location of the H-shell. This leads to an increase of CNO material, in particular ^{14}N in the envelope that could result in a rather normal thermal pulse evolution without any peculiar hydrogen convection zone. Whether the rotationally induced mixing processes before the AGB or the subsequent thermal pulse AGB evolution with the associated dredge-up events dominate the final CNO yields is not yet clear.

The difference between a real Pop III and an extremely metal-poor thermal pulse AGB star is the initial absence of Fe and other elements heavier than Al in the Pop III star. This does not preclude that a Pop III AGB stars can not generate *s*-process-elements by the slow neutron capture process. Goriely & Siess (2001) have used the *s*-process-framework established for solar-like metallicities (§ 7) and ran network calculations with an initial abundance appropriate for the interior of a $Z = 0$ TP-AGB star. They used the models of Siess et al. (2002) as stellar evolution input. The major uncertainty was the mixing for the formation of the neutron donor species ^{13}C , and the unknown feedback of such mixing to the thermodynamic structure evolution. Herwig (2004a) and Goriely & Siess (2004) have shown that this feedback is likely very important. Nevertheless, the *s*-process-models for $Z = 0$ are instructive, because they show that if a sufficient neutron source is available, the *s* process can be based on seed nuclei with lower mass number than Fe, for example C. C is produced in a primary mode in TP-AGB stars. For such a $Z = 0$ *s* process the Fe/Ni ratio should be markedly sub-solar, approximately close to the quasi steady-state value of ~ 3 , that is given by the ratio of the neutron cross sections of Ni and Fe (the isotopic minimum for each element). HE 0107-5240 with $[\text{Fe}/\text{H}] = -5.3$ (Christlieb et al., 2004) shows a larger than solar Fe/Ni ratio, which is evidence for the contribution of supernovae to the abundance distribution of this star.

3.2 The hydrogen-ingestion flash in ultra metal-poor or metal-free AGB stars

The peculiar H-convective episode described in the previous section was observed in AGB models with of $5 M_{\odot}$ and $Z = 0$ by Herwig (2003). During the following thermal pulse the He-shell flash convection zone reaches out into the H-rich envelope. This leads to the H-ingestion flash (HIF). Protons are mixed on the convective time scale into the He-shell flash region which is with depth increasingly hot. The hydrogen flash-burning leads to a separate convection zone as shown in Fig. 2. Convective H-burning in this layer is characterized by a large abundance of ^{12}C and protons. The protons have been mixed into this region from the envelope. Accordingly the ^{14}N abundance in this layer is very large, up to 10% by mass in a layer of $\approx 10^{-3} M_{\odot}$. The models show that after both the He-shell flash and the HIF have subsided a deep dredge-up episode will mix this ^{14}N -rich layer into the envelope. This may account for a substantial ^{14}N production and part of the observational pattern observed in EMP stars that are believed to be polluted by EMP AGB stars (§ 5). A HIF was also found in the $2 M_{\odot}$, $Z = 0$ model, but Herwig (2003) did not find the HIF in models of $Z \geq 10^{-5}$.

AGB stars are highly non-linear systems. The occurrence of the HIF depends on many details of the models, including the physics of mixing, opacities, the numerical resolution and nuclear reaction rates. Small changes in any of these ingredients, that may go unnoticed during a more robust stellar evolution phase (like the main-sequence), can be the deciding factor here whether a HIF occurs or not. Currently, theoretical models do not agree if and in which initial mass and metallicity regime the HIF occurs (Fujimoto et al., 2000; Chieffi et al., 2001; Siess et al., 2002; Herwig, 2003). However, it is important to better understand this situation because the HIF may play an important role in the *s* process in extremely metal-poor stars (Iwamoto et al., 2004). Hydrogen ingested into the He-shell flash or pulse-driven convection zone (PDCZ) may lead to ^{13}C production which could release neutrons. Suda et al. (2004) propose that the abundance pattern of the currently most metal-poor star – HE 0107-5420 – is in part due to the nucleosynthesis in a thermal pulse AGB star with HIF. The details of the nucleosynthesis in a HIF depend sensitively on the physics of simultaneous rapid nuclear burning and convective mixing. The hydrogen-ingestion flash can also be a source of lithium, distinctly different from conditions during hot-bottom burning (Herwig & Langer, 2001).

The evolution of born-again stars, like Sakurai’s object, provide valuable additional constraints with regard to the HIF in AGB stars (§ 6). The very late thermal pulse is associated with a HIF (Iben et al., 1983; Herwig et al., 1999). By reproducing the evolution of stars like Sakurai’s object one can gain some confidence in models of the HIF in metal-poor AGB stars. Herwig (2001) showed that models in which the convective hydrogen ingestion occurs with lower velocities than predicted by the mixing-length theory (Böhm-Vitense, 1958) feature a faster born-again evolution than MLT models, quantitatively in agreement with observations. The physical interpretation is that rapid

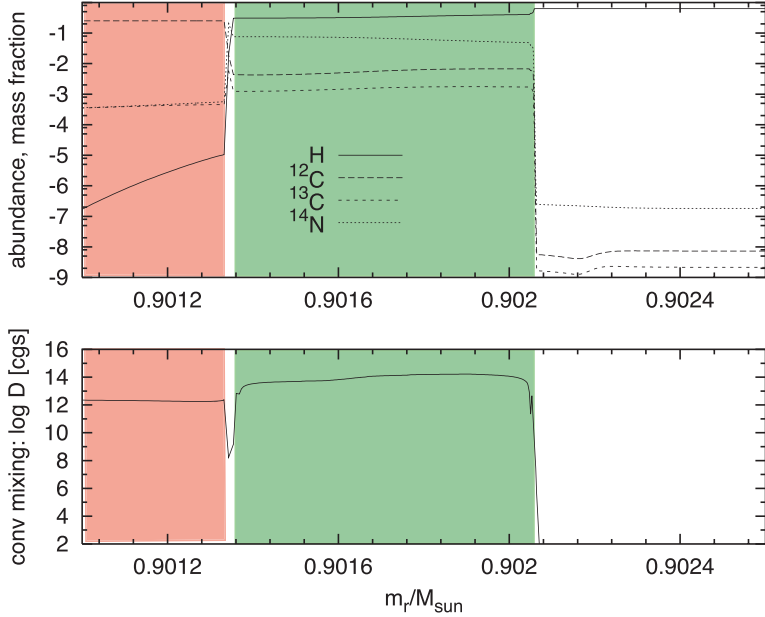


Figure 2: Burning and mixing in the H-ingestion flash during the 10th thermal pulse of a $5 M_{\odot}$, $Z = 0$ sequence (Herwig, 2003). Shown are the top layers of the He-shell flash convection zone (red), and the H-ingestion flash-driven convection zone (green). Top panel: abundance profiles; bottom panel: convective mixing coefficient.

nuclear burning on the convective time scale releases energy and adds buoyancy to down-flowing convective bubbles, leading to additional breaking of the plumes. The temperature and time scales for nucleosynthesis during the HIF would be significantly different. This has not yet been applied to HIF models at $Z = 0$ or extremely low metallicity.

3.3 AGB nucleosynthesis at extremely low metallicity

By definition all yields of Pop III stars are primary, because the initial composition contains only Big Bang material. Nuclear production is secondary when nuclei heavier than H and He are already present in the initial abundance distribution and transformed in other species. POP III or EMP AGB stars can produce a large number of species in primary mode, including the CNO elements, Ne, Na, Mg and Al. The production of heavier elements depends on the availability of neutrons. Some of these primary species, like oxygen, are usually not considered a product of AGB evolution at moderate metal-deficiency or solar metallicity. However, the initial envelope mass frac-

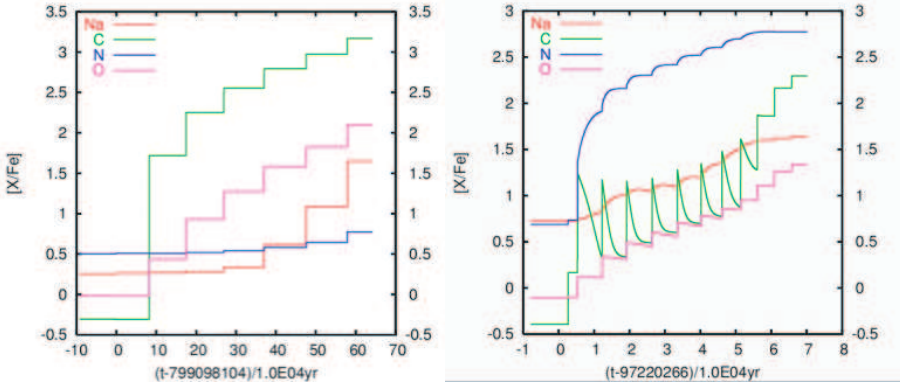


Figure 3: Surface evolution of C, N, O and Na for 2 and $5 M_{\odot}$ AGB evolution models at $[Fe/H] = -2.3$ (Herwig, 2004b). The ejecta of the $2 M_{\odot}$ case are released after 0.8Gyr, whereas the $5 M_{\odot}$ case releases the ejecta after 0.1Gyr. The abundance evolution is determined by the interplay of dredge-up and hot-bottom burning. Each step in the curves corresponds to a dredge-up event after a thermal pulse. Hot-bottom burning can be observed in the $5 M_{\odot}$ case as the decrease of C and increase of N (and to a lesser extent Na) inbetween dredge-up events. Note the dichotomy in the C/N ratio in the low-mass vs. high-mass AGB star.

tion of oxygen for models with $Z = 10^{-4}$ is $< 5 \cdot 10^{-5}$. ^{16}O in the intershell material (cf. Fig. 6) that is dredged-up is primary and even at this low metallicity of the order 1% by mass. Dredge-up of such material will enhance the envelope abundance significantly.

A set of low- and intermediate mass AGB stellar evolution models with $Z = 10^{-4}$ ($[Fe/H] = -2.3$) with detailed structure, nucleosynthesis and yield predictions has been presented by Herwig (2004b). The oxygen overabundance in these models is $\log(X/X_{\odot}) = 0.5 \cdots 1.5$, depending on mass. The abundance evolution for C, N, O and Na is shown in Fig. 3 for two initial masses. The evolution of C and N is qualitatively different in the two cases. The lower mass sequence shows the increase of C and some O due to the repeated dredge-up events. No significant amount of ^{14}N is dredged-up. The result is a large C/N ratio. The $5 M_{\odot}$ track shows the opposite behaviour. The much lower C/N ratio is the result of hot-bottom burning (Boothroyd et al., 1993). C and O are dredged-up after the thermal pulse as in the lower mass case, but during the following quiescent interpulse phase the envelope convection reaches into the region hot enough for H-burning and the envelope C is transformed into N. The initial-mass transition between hot-bottom burning models with large N abundances and C dredge-up models without hot-bottom burning is very sharp. This precludes the notion that EMP stars with simultaneously large N and C overabundances, like CS 29497-030 with $[C/Fe] = 2.4$ and $[N/Fe] = 1.9$ (Sivarani et al., 2004), may be polluted by such AGB stars in the transition

regime where hot-bottom is only partially efficient (see § 5).

The signature of hot-bottom burning in Fig. 3 is a gradual change of abundance between the steps caused by dredge-up. From this it can be seen that Na has a different nuclear production site depending on initial mass. In the $2 M_{\odot}$ case Na is produced in the He-shell flash, by n-captures on ^{22}Ne . The neutrons come from the $^{22}\text{Ne}(\alpha, n)$ reaction. ^{23}Na is the dredged-up but not produced during the interpulse phase. The neutron-heavy Mg isotope ^{26}Mg is produced in a similar way. In the $5 M_{\odot}$ case Na is mainly produced in hot-bottom burning, by p-capture on dredged-up ^{22}Ne .

In the previous section it was argued that due to the large primary production of CNO and many other species the $Z = 0$ model predictions would also apply approximately to stars with ultra-low metallicity as well. Neutron capture reactions play an important role, and need to be included in yield-predictions, together with a neutron-sink approximation for species not explicitly included in the network. This has been done in a qualitatively similar way by both Herwig (2004b) for the $Z = 10^{-4}$ models and Siess et al. (2002) for their $Z = 0$ models, and the abundance evolution is quantitatively similar. Both model sets predict for non-hot-bottom burning cases large primary production of C and O, while the ^{14}N abundance does not change. ^{22}Ne is produced in both cases in the He-shell flashes, and in both cases the final ^{22}Ne exceeds that of ^{14}N . The evolution of ^{23}Na , ^{25}Mg and ^{26}Mg is qualitatively the same too. In particular the ratio of these three isotopes is quantitatively the same in the last computed model of the $Z = 0$ sequence and the final AGB model at $Z = 10^{-4}$. This is in particular interesting as these low-mass AGB models predict that $^{26}\text{Mg} : ^{25}\text{Mg} > 1$, contrary to the signature of hot-bottom burning.

One of the largest uncertainties is the adopted mass loss. While mass loss in AGB stars of solar metallicity can be constraint observationally, this has not been possible for extremely low metallicity. Other uncertainties relate to mixing in EMP AGB stars. Herwig (2004a) has shown that convection induced extra-mixing, like exponential overshoot that is used to generate a ^{13}C pocket for the *s*-process in higher-metallicity models, may lead to vigorous H-burning during the third dredge-up. Depending on the efficiency of such mixing the third dredge-up may turn into a flame-like burning front, leading to very deep core penetration. This may significantly impact the formation and effectiveness of a ^{13}C pocket for the *s* process (Goriely & Siess, 2004).

4 Near-field cosmology application of stellar yield calculations

Accurate stellar yields for intermediate mass stars are requested by another emerging field, near-field cosmology (Bland-Hawthorn & Freeman, 2000; Freeman & Bland-Hawthorn, 2002). The baryon (stellar) halo of the Milky Way retains a fossil imprint of the merging history of the galaxy. Different merging components, like the infalling dwarf galaxies with a range of masses, have different star formation

histories that translate into different abundance signatures of the member stars of these components. The current surge of spectroscopic multi-object capabilities at large telescopes will likely significantly enhance the importance of this approach.

An example is the recent work by Venn et al. (2004) in which abundances of halo stars are compared with abundances of stars in satellites, dwarf galaxies trapped in the potential well of the Galaxy. Here, the basic idea is that dwarfs are merging with a galaxy at different times at which point star formation and chemical evolution stops. Satellites that survive until the present day should show the signature of more evolved chemical evolution, for example including the *s*-process elements associated with the long-lived low-mass stars. In contrast, halo stars that are the dispersed members of dwarf galaxies that have merged at an earlier time in the evolution of the galaxy, have less evolved chemical evolution patterns, for example showing more clearly the patterns of nucleosynthesis in massive star evolution.

Potentially, the implications that can be derived from comparison of halo stars and satellite members may include some fundamental questions of nucleosynthesis itself. The data presented in Venn et al. (2004) show that $[\alpha/\text{Fe}]$ is systematically smaller in stars belonging to satellites compared to their halo counterparts. This can be explained in the Λ cold dark matter model that predicts that most halo stars have formed in rather massive dwarf galaxies, which merged with the galaxy a long time ago (Robertson et al., 2005). These stars show the signature of truncated chemical evolution, dominated by the yields of supernovae type II and their significant α -element contribution and moderate Fe ejecta. Stars in present, less massive satellite galaxies show the signature of chemical evolution components that take more time, like the SN Ia. These events add Fe but little α -elements, and their $[\alpha/\text{Fe}]$ ratio is therefore smaller.

Abundances of other elements could be compared too. For example, Venn et al. (2004) compare among others the abundances of Y, Ba and Eu in halo stars and satellite dwarf galaxies. Ba is typically considered an main-component *s*-process element (at least at $[\text{Fe}/\text{H}] > -2$) because the elemental solar abundance has a 81% *s*-process contribution (Arlandini et al., 1999). Only the smaller remaining fraction is made in the r-process. As discussed above, the nuclear production site of the main-component of the *s*-process are low- and intermediate mass AGB stars, in the initial mass range $1.5 < M_{\text{ini}}/\text{M}_\odot < 3.0$. This component of galaxy chemical evolution needs even more time to contribute than the SN Ia. And indeed, $[\text{Ba}/\text{Fe}]$ behaves differently from $[\alpha/\text{Fe}]$ in halo stars and satellite stars. $[\text{Ba}/\text{Fe}]$ is on average higher in the satellite stars than in halo stars, with a considerable spread. This is consistent with the framework of truncated chemical evolution of systems that were early disrupted in merger events, and with the understanding of stellar evolution and nucleosynthesis that α -elements are predominantly made in short-lived massive stars, while Ba originates in rather old populations. It is then extremely interesting to consider the r-process element Eu, which in the solar abundance distribution has a very small *s*-process contribution of

only 5.8%. This element does not behave like α -elements. Instead, [Eu/Fe] is on average the same in halo stars and dwarf galaxy stars, however with a larger spread in the latter. In order to remain in the proposed scenario of why abundances in the halo differ from those in the nearby dwarf galaxies one would then have to assume that at least an important fraction of the r-process elements does not originate in SN II, which eject their yields on a short time scale. Instead, one would have to assume that Eu in the satellite stars comes from a source that releases the ejecta on a time scale comparable to or longer than the Fe production in SN Ia. Such sources could be the accretion induced collapse (Fryer et al., 1999) or the collapse of a super-AGB star in the initial mass range $8 \dots 10 M_{\odot}$, if the core mass grows to the Chandrasekhar limit (Nomoto, 1984). It would certainly go to far at this point to draw any further conclusion, for example in conjunction with the two r-process source model proposed by Qian & Wasserburg (2003).

It is clear, that the full potential of using the abundances patterns of stars to reconstruct the formation of galaxies in their cosmological context can only be reached with detailed yield predictions including all masses and reaching down to extremely low metallicity. Y is another example that reinforces this notion. In the solar abundance distribution it has a 92% fraction from the main-component *s*-process originating in low-mass stars. However, it is also the termination point of the weak *s*-process from massive stars, and it does have some r-process contribution. In the data presented by Venn et al. (2004) it behaves – with regard to the difference between halo and satellite stars – like the α -elements, which in this context would imply an important contribution from massive stars.

5 The origin of nitrogen in the early universe

Nitrogen is the fifth most common element in the universe. In stellar evolution of very low metallicity the primary production is of particular importance. Strictly from a nucleosynthesis point of view nitrogen is always made in a well established sequence of events, involving first the triple- α process that makes ^{12}C and then two subsequent proton captures that are part of the CN-cycle. In a stellar model sequence the problem is to identify the mixing processes that can account for this sequence of events. How can ^{12}C , that is made in the He-burning that requires higher temperatures, be brought into layers of lower temperature where H-burning still takes place. Or, how can protons be mixed down into the He-burning layers and be captured by ^{12}C to eventually form ^{14}N , but then not be exposed to α -captures that would convert ^{14}N into ^{22}Ne . Because the primary production of nitrogen depends so much on stellar mixing, this element assumes a key role in understanding stellar nucleosynthesis at extremely- and ultra-low metallicity.

Nitrogen is certainly present in the most metal-poor stars in the Milky Way (Laird, 1985). According to standard stellar evolution and nucleosynthesis models primary N comes from intermediate mass (IM) AGB stars

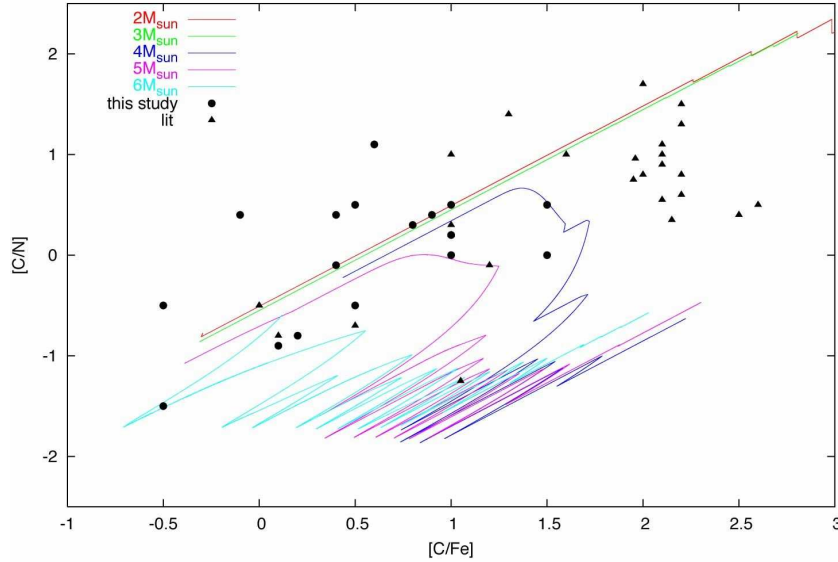


Figure 4: Observed nitrogen and carbon abundances (including literature data from Barbuy et al., 1997; Preston & Sneden, 2001; Aoki et al., 2001; Lucatello et al., 2003) compared to the surface abundance evolution of AGB model tracks.

(Herwig, 2004b), with perhaps a small contribution from rotating massive stars (Meynet & Maeder, 2002). In AGB stars the repeating sequence of thermal pulses induce convective mixing events that lead to the production of N. C is made in the He-shell flash. Dredge-up after the flash mixes that C into the envelope, and in massive AGB stars the C in the envelope is then transformed into N. The low $[N/\alpha]$ abundances observed in some damped Lyman- α systems (Pettini et al., 1999) have prompted suggestions that the IMF may be biased in favor of massive stars in some systems (Prochaska et al., 2002), or that these systems represent the earliest stages of chemical evolution of massive stars only (Centurión et al., 2003).

Observations of N and C abundances in C-rich EMP stars with *s*-process-signature provide another way to study the N production at low metallicity. About 30% of all extremely metal-poor stars ($[Fe/H] \approx -2$) are strongly C- and to a lesser extent N-enhanced (§ 2). In particular the overabundance of C and of N in addition to their *s*-process signature has lead to the assumption that the AGB star progenitor of the current white dwarf companion to the CEMP-*s* star is responsible for the observed abundance pattern. Because of the established binary nature and the *s*-process-signature the CEMP-*s* stars are assumed to be polluted by the individual AGB stars that are the progenitors of their present white dwarfs companions.

In Fig. 4 the $[C/N]$ and $[C/Fe]$ ratios of literature data are shown, together

with the AGB model prediction of $2 - 6 M_{\odot}$ tracks. The literature data show systematically lower [C/N] ratios than what is expected by 2 or $3 M_{\odot}$ models that dredge-up C, but do not produce N. This poses the question of the primary origin of the N in these stars.

Models of initial masses between 4 and 6 feature efficient hot-bottom burning (HBB) which turns most dredged-up primary carbon into nitrogen resulting in $[C/N] \sim 1$ and $[C/Fe] \sim 1.5$. However, none of the literature data seem to show the very low [C/N] ratio that would be expected for an EMP star that happened to have an AGB companion in the $4 - 6 M_{\odot}$ initial mass range. We have carried out observations of EMP targets with $0.5 < [C/Fe] < 1$ using the CH and the NH band for abundance determination (Johnson et al., 2005; Herwig et al., 2004). Specifically we wanted to find out whether the paucity of EMP stars with $[C/N] \sim 1$ is a selection effect or a systematic observational bias imposed by the abundance indicators employed in previous studies. While C-strong stars can be identified by the G-Band at 4305\AA , the strong NH band at 3360\AA is never observed in the medium-resolution surveys that provide the targets for detailed abundance studies (e.g. Beers et al., 1992). Only the CN bands at 3883\AA and 4215\AA are included, and CN lines are not strong in N-rich stars unless C is also enhanced by a large amount. Therefore, studies of C and N abundances have favored C-rich stars that are easily identified, and may have missed stars that have $[C/Fe] \sim 0 - 1$, but are more rich in N. Thus the literature data in Fig. 4, drawn from high-resolution follow-up of the medium-resolution candidates, may be the result of a strong observational bias against finding N-rich stars.

In order to overcome this bias we obtained spectra for 18 new stars. In Fig. 4, we plot the preliminary estimates of the [C/N] ratios of 18 stars, based on observations of the NH bands during 6 nights at CTIO/KPNO. We did not find any stars with low [C/N], and the analysis of additional data is underway to put our findings on a more robust statistical basis. This leaves us with two important open questions: (1) Where are the EMP stars polluted by massive AGB stars? and (2) Where does the N in the CEMP stars come from that we do observe? While we do not have any idea at this point of what the answer to the first question could be, there are a number of possibilities to address the absence of primary N. These include rotationally induced mixing before the AGB phase (§ 3.1), the H-ingestion flash (§ 3.2), and extra-mixing in AGB stars (Nollett et al., 2003) as envoked in models of RGB stars to account for abundance anomalies in globular cluster member stars (Denissenkov & Vandenberg, 2003). In any of these cases the interpretation of N abundances in metal-poor systems of all kinds may have to be re-evaluated.

6 H-ingestion flash and born-again evolution

Nuclear production in the AGB stellar interior can become observable at a later time in the evolution, during the post-AGB phase, on the surface of those

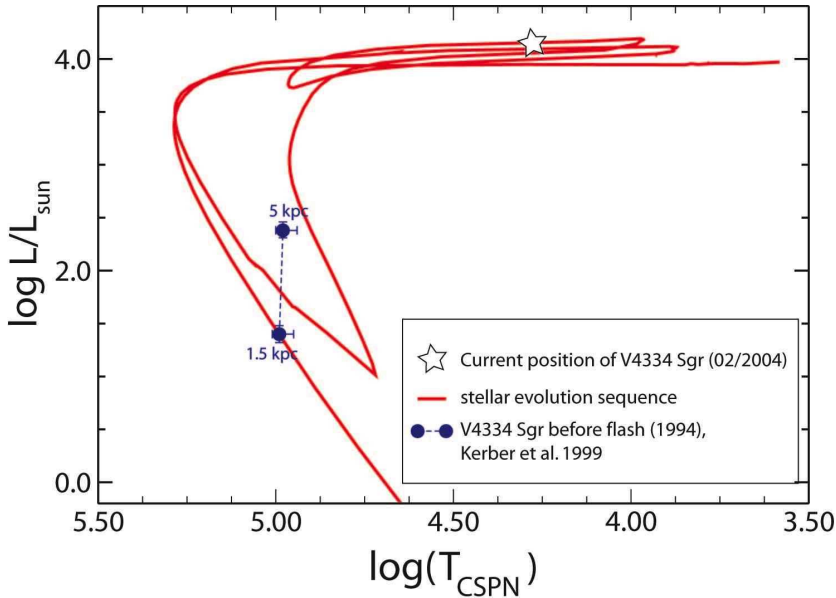


Figure 5: Observational position of Sakurai’s object (V4334 Sgr) at different times, and evolutionary sequence of a $0.604 M_{\odot}$ central star of a planetary nebula track (Hajduk et al., 2005) with a very late thermal pulse (H-ingestion flash) with modified convective mixing velocities according to Herwig (2001).

central stars of planetary nebulae that become H-deficient. Here H-deficient means in most cases that the mass fraction of H as observed in the stellar spectrum is less than $\approx 2\%$. This leads to additional important constraints on the evolution of AGB stars, which is in particular important to study AGB evolution at extremely low metallicity.

H-deficient central stars of planetary nebulae (CSPN) as well as very young white dwarfs have been analysed in detail (e.g. Koesterke, 2001; Werner, 2001; Hamann et al., 2003) and new important information about the abundances of these stars is yet to be revealed. Stellar evolution predicts that about 25% of all post-AGB stars will eventually loose all their small remaining H-rich envelope mass of the order $10^{-4} M_{\odot}$ and expose the bare H-free cores. The carbon, oxygen and helium rich nature of these objects is evident from their Wolf-Rayet or PG 1159 type emission line spectra, and reflects nuclear processed material that has been built up during the stars progenitor evolution. Although there is considerable spread in the observed abundances of these stars, the pattern can be summarized in mass fraction as $\text{He} \sim \text{C} \sim 0.4$ and $\text{O} = 0.08 \dots 0.15$.

These H-deficient CSPN are important for AGB evolution modeling, because they provide a unique opportunity to study directly the nuclear processing shells in AGB stars. In order to explain the evolutionary origin Iben et al.

(1983) introduced the born-again evolution scenario . The star evolves off the AGB, and becomes a hydrogen-rich central star and eventually a very hot, young white dwarf. However, the He-shell may still be capable to ignite a late He-shell flash, and in that case the star retraces its evolution in the HRD, back into the giant region (Fig. 5). As a result of hydrogen-ingestion into the He-convection and rapid burning, or by mixing from the emerging convective envelope (or because of both) the surface abundance of such born-again stars will be extremely H-deficient or even H-free.

Stellar models of this evolutionary origin scenario connect the surface abundance of the Wolf-Rayet central stars and the PG1159 stars with the intershell abundance of the progenitor AGB star. The intershell layer between the He- and the H-shell is well mixed during each He-shell flash. This zone contains the main nuclear production site of the progenitor AGB star, and the abundance of this zone reflects contributions from both He- and H-shell burning (Fig. 6). As a result of the born-again evolution these layers become visible at the surface of the resulting H-deficient CSPN.

The initial models of the H-deficient central stars by Iben and collaborators showed qualitatively that the born-again scenario could account for high He and C abundances, as these elements were abundant in the intershell of the AGB progenitor model they used. However, they could not account for the high observed oxygen abundance. Herwig et al. (1997) were the first to propose that the solution could be non-standard mixing during the AGB evolution. Models with overshooting at the bottom of the pulse-driven convection zone do not only feature higher temperatures at the bottom of that layer (§ 7.1), but they also show higher C and in particular O abundances in the PDCZ. Subsequently, Herwig (2000) has explored in detail how the various abundances depend on the overshoot efficiency and other details. In essence, overshooting brings AGB intershell abundances of He, C and O in very good quantitative agreement with the observed abundances of Wolf-Rayet type central stars and PG1159 stars, in the framework of the born-again evolution. More effort is needed to consolidate these constraints on the intershell abundance with the possibly tight upper limits on overshooting at the bottom of the PDCZ that the *s* process may provide (§ 7.1).

The connection of the surface abundances of the hot PG1159 stars and the progenitor AGB intershell abundance has been reinforced recently by several new observational findings. These include a substantial overabundance of Ne (Werner et al., 2004), F abundances ranging from solar up to 250 times solar (Werner et al., 2005) in good agreement with AGB nucleosynthesis predictions by Lugaro et al. (2004), and Fe-deficiencies of at least 1 dex compared to solar (Miksa et al., 2002), which may reflect the depeletion of Fe in the AGB intershell due to *s*-process n-captures. In that case the Fe/Ni ratio should be low, as in fact observed in Sakurai's object. This born-again star is the smoking gun of the very late thermal pulse scenario and links this evolutionary scenario with the H-deficient PG 1159 and Wolf-Rayet type central stars (Duerbeck et al., 2000; Herwig, 2001). Much of the observed abundance pattern of Sakurai's object as well as the rapid evolutionary time scale has been

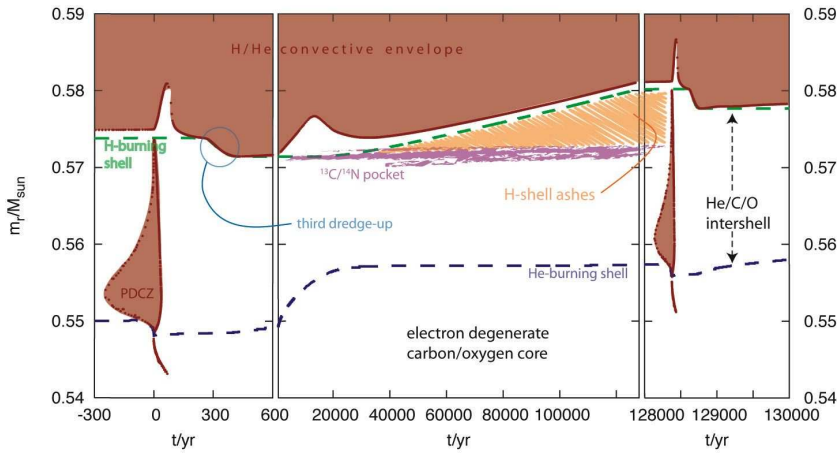


Figure 6: Evolution of convection zones (red regions) and burning shells (dashed lines) in 1D stellar track including two He-shell flashes and the quiescent H-burning phase inbetween. The purple indicates the location of the ^{13}C -rich region that contains the bulk s -process-production. The orange region contains the ashes of the H-shell that are engulfed by the following He-shell flash convection zone.

reproduced quantitatively with stellar models (Asplund et al., 1999; Herwig, 2001). Similar to the PG 1159 stars, Sakurai's object shows Fe depletion of about 1dex compared to solar. The low ratio of $(\text{Fe}/\text{Ni}) = 3$, shows that Sakurai's object shows surface material that has been directly irradiated with neutrons (Herwig et al., 2003b). New radio observations show that Sakurai's object has started reheating again, on its second evolution into the CSPN (Hajduk et al., 2005). This marks a new phase of the evolution of this star, and confirms the concept of convective mixing efficiency modified by nuclear burning (Herwig, 2001).

7 s process and AGB stars

The s process is the origin of half of all elements heavier than iron (Arlandini et al., 1999). It is also important for isotopic ratios and in some cases elemental abundances of lighter elements - in particular at extremely low metallicity. The heavy elements are made by the s process through neutron captures that are slow compared to the competing β -decay. Starting from the abundant iron group elements it follows closely the valley of stability in the chart of isotopes. It is characterized by neutron densities $N_n < 10^{10}\text{cm}^{-3}$. Observations and theory agree that the nuclear production site of the main and strong component of the s process ($90 < A < 204$) originates in low mass Asymptotic Giant Branch (AGB) stars. The weak component below the first s -process peak at $A = 90$ is produced during He and C burning in massive

stars. Here we deal only with the *s*-process in AGB stars.

The *s*-process is important in the context of the second stars for two reasons. First, the observed elemental abundance distribution of the trans-iron elements is at any given metallicity a mix of *s*- and *r*-process contribution. In order to disentangle the two contributions in very-low metallicity stars, the *s*-process in this metallicity regime needs to be understood. This may than enable progress in identifying the conditions for the *r*-process. Second, *s*-process-branchings can be used to probe the physics for stellar mixing (§ 7.2), which is particularly usefull when modeling the evolution of EMP stars.

The *s* process in low-mass AGB stars has two neutron sources. The main source is ^{13}C , that forms via the $^{12}\text{C}(\text{p}, \gamma)^{13}\text{N}(\beta^+)^{13}\text{C}$ reaction. At the end of the dredge-up phase (Fig. 6) after the He-shell flash, when the bottom of the H-rich convective envelope has penetrated into the ^{12}C rich intershell layer, partial mixing at this interface would create a thin layer providing simultaneously the required protons and ^{12}C . The *s* process in the ^{13}C pocket is characterized by low neutron densities ($\log N_{\text{n}} \sim 7$) that last for several thousand years under radiative, convectively stable conditions during the quiescent interpulse phase. The physics of mixing at the H/ ^{12}C interface at the end of the third dredge-up phase has not yet been clearly identified (see below). Most likely it is some type of convection induced mixing beyond the convection boundary.

The $^{22}\text{Ne}(\alpha, \text{n})^{25}\text{Mg}$ reaction requires the high temperatures that can be found at the bottom of the pulse-driven convection zone (PDCZ) during the He-shell flash ($T > 2.5 \cdot 10^8$ K). The neutrons are released with high density ($\log N_{\text{n}} \sim 9 \dots 11$) in a short burst (Gallino et al., 1998). These peak neutron densities are realised for only about a year, followed by a neutron density tail that lasts a few years, depending on the stellar model assumptions. The current quantitative modeling of the *s*-process uses the thermodynamic output from a stellar evolution calculation including mass loss as input for nucleosynthesis calculations with a complete *s*-process network Busso et al. (1999). The post-processing accounts for both the ^{13}C neutron source as well as for the ^{22}Ne source, and mixes the different contributions according to the information provided by the stellar evolution calculations. The free parameter of the model is the ^{13}C abundance in the ^{13}C pocket that is proportional to the neutron exposure that results from burning the ^{13}C in the (α, n) reaction. Physical mixing processes which are responsible for bringing protons down from the envelope into the ^{12}C -rich core to enable ^{13}C formation, are not explicitly included in this model.

Observationally, models have to account for observed spread in observables that are related to the neutron exposure (e.g. Van Winckel & Reyniers, 2000; Eck, S. van & eta., 2003; Nicolussi et al., 1998). This spread is not only evident from stellar spectroscopy, but also from SiC grain data, that indicate that a spread by a factor of five is necessary for the neutron exposure for a given mass and metallicity (Lugardo et al., 2003a). Currently, this spread is accounted for by a range of different cases in each of which the ^{13}C abundance

in the pocket is assumed to be different (Busso et al., 2001). However, the physics of the mixing that is associated with the range of neutron exposures has yet to be identified.

7.1 Convection and rotationally induced mixing for the *s* process

It is useful to distinguish *s*-process-mixing for solar and moderately metal-poor stellar evolution, and the extremely and ultra metal-poor cases. In the first, the assumption that *s*-process-mixing does not feedback strongly into the thermodynamic evolution is generally valid, in the latter it is generally not. Many more observational constraints exist for the solar and moderately metal-poor *s* process, in particular the isotopic information from the pre-solar SiC grains.

Mixing for the for the solar and moderately metal-poor *s* process has to satisfy two general constraints: (1) How is the partial mixing zone of H and ^{12}C generated that eventually forms the neutron source species ^{13}C , and (2) what is the origin of the observed spread in neutron exposures. Mixing for the ^{13}C pocket is probably related to the penetrative evolution of the bottom of the convective envelope during the third dredge-up. Possible mechanisms include exponential diffusive overshooting (Herwig et al., 1997; Herwig, 2000), mixing induced by rotation (Langer et al., 1999), and mixing by internal gravity waves (Denissenkov & Tout, 2003). Each of these effectively leads to a continuously and quickly decreasing mixing efficiency from the H-rich convection zone into the radiative ^{12}C -rich layer, and each of these will lead to the formation of two pockets which are overlapping (Lugardo et al., 2003b). At low H/ ^{12}C ratios H-burning is proton-limited, and protons will make ^{13}C via the $^{12}\text{C}(\text{p},\gamma)$ reaction but no (or little) ^{14}N . At larger H/ ^{12}C ratio a ^{14}N pocket forms. The maximum abundance of both ^{13}C and ^{14}N depends on the ^{12}C abundance in the intershell. Therefore, the conditions in the ^{13}C pocket are not independent of, for example, the mixing at the bottom of the PDCZ. Lugardo et al. (2003b) derive the relationship $\tau_{\max} = 1.2X(^{12}\text{C})_{\text{IS}} + 0.4$, where $X(^{12}\text{C})_{\text{IS}}$ is the intershell ^{12}C mass fraction and τ_{\max} is the maximum neutron exposure reached in the ^{13}C pocket. The observations of H-deficient post-AGB stars described in § 6 require that the ^{12}C abundance in the PDCZ of AGB stars is about 40%. This value is reproduced in AGB stellar evolution models with overshooting at the bottom of the PDCZ, and about twice as large as in models without overshooting.

Apart from the maximum amount of ^{13}C in the pocket the mixing process must produce a partial mixing layer of the right mass ΔM_{spr} which eventually contains *s*-process enriched material. In the exponential overshooting model of Herwig et al. (1997) the mixing coefficient is written as $D_{\text{OV}} = D_0 \exp\left(\frac{-2z}{f_{\text{ov}} \cdot H_p}\right)$, where D_0 is the mixing-length theory mixing coefficient at the base of the convection zone, z is the geometric distance to the convective boundary, H_p is the pressure scale height at the convective boundary, and

f_{ov} is the overshooting parameter. If applied to core convection $f_{ov} = 0.016$ reproduces the observed width of the main sequence. Lugaro et al. (2003b) finds that $f_{ov} = 0.128$ at the bottom of the convective envelope generates a large enough ^{13}C pocket. However, the maximum neutron exposure in the ^{13}C pocket of the overshooting model is $0.7 \cdots 0.8 \text{mbarn}^{-1}$, while in the non-overshooting models this value is 0.4mbarn^{-1} . Correspondingly Lugaro et al. (2003b) obtained only negative values for the logarithmic ratio $[\text{hs}/\text{ls}]^1$, while the overshooting model with the larger neutron exposure predicts $[\text{hs}/\text{ls}] \sim 0$. This compares to an observed range of $-0.6 < [\text{hs}/\text{ls}] < 0.0$ for stars of solar metallicity (see Busso et al., 2001, for a compilation of observational data). Models with overshooting at all convective boundaries can reproduce only the largest observed hs/ls ratios, indicating that the neutron exposure in the ^{13}C pocket in these models is at the maximum of the observationally bounded range.

Overshooting alone is not able to account for all features of *s*-process-mixing. In particular there is no mechanism to account for the spread in neutron exposures within the overshooting framework. Rotation, however, may induce a range of mixing efficiencies for a sample of stars with otherwise identical parameters. Models of rotating AGB stars were presented by Langer et al. (1999), and the *s* process was analyzed in detail by Herwig et al. (2003a) and Siess et al. (2004). The implementation of rotation for the AGB models was the same as the one that had been used previously to construct rotating models of massive stars (Heger et al., 2000). This implementation yields a ^{13}C pocket generated by shear mixing below the envelope convection base, however an order of magnitude smaller than what is needed in the partial mixing zone of a non-rotating model to reproduce the observed over-production in stars. The second important finding is that shear mixing which initially generates the small ^{13}C pocket, prevails throughout the interpulse phase, even when the base of the convection is receding in mass after H-shell burning has resumed. When the dredge-up ends, the low-density slowly rotating convective envelope and the fast rotating compact radiative core are in contact and mixing is induced through shear at this location of large differential rotation. This radial velocity gradient remains as a source for shear mixing at exactly the mass coordinate of the ^{13}C pocket with important consequence for the *s*-process. Shear mixing during the interpulse phase swamps the ^{13}C pocket with ^{14}N from the pocket just above. By the time the temperature has reached about $9 \cdot 10^7 \text{K}$ and ^{13}C starts to release neutrons via $^{13}\text{C}(\alpha, n)^{16}\text{O}$, ^{14}N is in fact more abundant than ^{13}C in all layers of the ^{13}C pocket. ^{14}N is a very efficient neutron poison. It has a very large $^{14}\text{N}(n, p)^{14}\text{C}$ rate and simply steals neutrons from the iron seed. As a result, the neutron exposure is only $\sim 0.04 \text{mbarn}^{-1}$, about a factor of ten too small to generate the observed *s*-process abundance distribution. The detailed post-processing models of current rotating AGB stars showed that they are not capable to

¹hs and ls are the heavy and light *s*-process-indices which are the average of the abundances of elements around the neutron magic numbers 50 and 80.

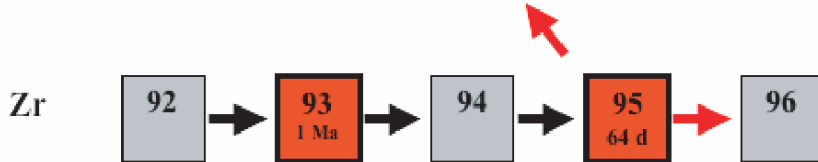


Figure 7: Small section of the chart of nuclides, showing the branching at ^{95}Zr . The s process proceeds by adding neutrons to both stable (grey) and unstable (red) species. Radioactive species like ^{95}Zr can either β -decay or capture a neutron.

account for the observed s -process overabundances. Parametric models show that weaker shear mixing during the interpulse leads to a weaker poisoning effect. For very small poisoning effects the neutron exposures are still large enough to reproduce some observations.

While neither rotation or overshooting alone provide the right amount of s -process-mixing it is interesting to consider a combination of these. In essence the idea is that overshooting would provide mixing for the formation for the ^{13}C pocket and for a larger ^{12}C abundance in the PDCZ to obtain a large neutron exposure in the ^{13}C pocket. Then, shear mixing during the interpulse could add some poison and result in the observed spread. Magnetic fields have not yet been considered in AGB stellar evolution. However, one may assume that qualitatively magnetic fields will add coupling between the fast rotating core and the slowly rotating envelope and provide additional angular momentum transport. Models including this effect could result in smaller shear mixing than predict by the current rotating AGB stellar models.

It is interesting to note that such an effect of magnetic fields may also help to reconcile the predicted rotation rates of AGB cores of $\sim 30\text{km/s}$ with the rotation rate determinations of white dwarfs. Spectroscopic determinations of rotation rates of white dwarfs of spectral type DA can not rule out such values, but most are also consistent with zero or very low rotation (Koester et al., 1998; Heber et al., 1997). However, asteroseismological measurements of WD rotation rates clearly yield smaller values in the range $0.1 < v_{\text{rot}}/(\text{km/s}) < 1$ (see references in Kawaler, 2003).

7.2 s process as a diagnostic tool

The high precision information on the pre-solar meteoritic SiC grains provide isotope ratio measurements that allow to probe the conditions at the s -process nuclear production site in more detail. One example is the highly temperature dependent nucleosynthesis triggered by the release of neutrons from ^{22}Ne at the bottom of the PDCZ. The temperature at the bottom of the PDCZ correlates with the efficiency of extra mixing like overshooting at the bottom of this convection zone (Herwig, 2000). Neutrons in the PDCZ are generated by the $^{22}\text{Ne}(\alpha, n)^{25}\text{Mg}$ reaction. For larger temperatures the neutron

density is higher. Isotopic ratios that enclose a branch point isotope in the *s*-process path will be more neutron heavy for higher neutron densities. An example is the $^{96}\text{Zr}/^{94}\text{Zr}$ -ratio, that is set by the branching at the radioactive ^{95}Zr (Fig. 7). For low neutron densities ^{95}Zr decays. For $N_{\text{n}} > 3 \cdot 10^8 \text{ cm}^{-3}$ $^{95}\text{Zr}(n, \gamma)^{96}\text{Zr}$ becomes significant, hence ^{96}Zr is produced. If the temperature is larger the neutron density is larger and the $^{96}\text{Zr}/^{94}\text{Zr}$ ratio, which can be measured in SiC grains, is larger as well.

Lugardo et al. (2003a) have studied the measured isotopic ratios of Mo and Zr as well as Sr and Ba from SiC grains. They evaluate the sensitivity of their results in terms of nuclear reaction rate uncertainties. All branchings that are activated by the ^{22}Ne neutron source depend on the still uncertain $^{22}\text{Ne}(\alpha, n)^{25}\text{Mg}$ rate. In addition, the $^{96}\text{Zr}/^{94}\text{Zr}$ ratio depends on the neutron cross-section of the unstable isotope ^{95}Zr . Like for almost all radioactive nuclei the (n, γ) rate of ^{95}Zr is not measured. The theoretical estimates vary from Maxwellian-averaged cross sections of 20mb (Beer et al., 1992) to 140mb (JENDL-3.2). In order to make full use of the potent method of using the *s* process as a diagnostic tool it is critical that n-capture rates of the radioactive *s*-process-branch point nuclides are measured. Different *s*-process-branchings are sensitivity to different mixing processes, including those that may be induced by rotation.

The *s*-process as a diagnostic tool can provide information on mixing processes that are potentially relevant for the evolution of stars of all masses, including the progenitors of supernovae. In particular the details of the initial model for a supernova calculations determines important properties of the explosion, like asymmetries, or the final fate as black hole or neutron star (Young et al., 2005).

8 Carbon star formation and nuclear reaction rate input

In order to understand C-rich extremely metal-poor (CEMP) stars the formation of C-rich AGB stars has to be understood in a quantitative way. AGB stars become C-rich because of the third dredge-up, which mixes C-rich material from the intershell into the envelope (Fig. 6). The evolution of C and O in AGB stars and the problems related to modelling the third dredge-up are discussed in Herwig (2005). In summary, the third dredge-up is now obtained in 1D stellar evolution calculations in sufficient amount and at sufficient low core mass. These calculations take into account convection-induced mixing into the stable layers in a time- and depth dependent way, and use high numerical resolution. Uncertainty is introduced by the mixing length parameter (Boothroyd & Sackmann, 1988).

Understanding the dredge-up properties of AGB stars is important, because the dredge-up dependent yield predictions for low and intermediate mass stars enter models for galaxy chemical evolution. AGB stars serve as diagnostics for extragalactic populations, and for this purpose the conditions

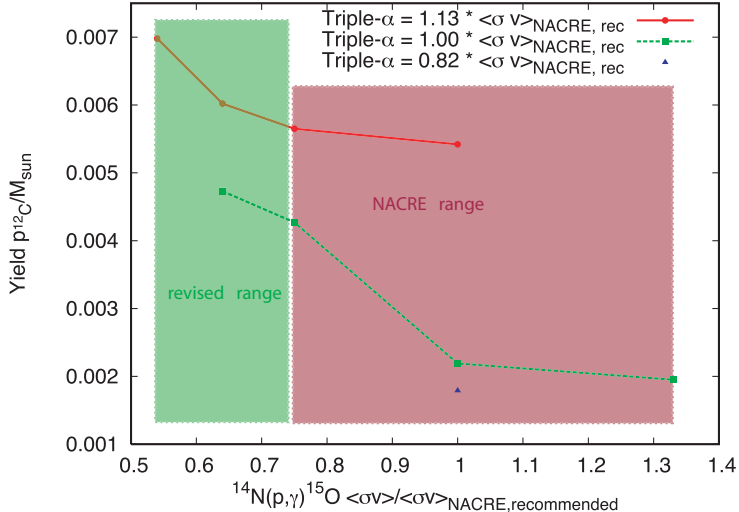


Figure 8: Carbon yield as a function of nuclear physics input. Each point gives the yield. from one full $2 M_{\odot}$, $Z = 0.01$ TP-AGB stellar evolution sequence with the indicated choice for the ${}^{14}\text{N}(\text{p}, \gamma){}^{14}\text{O}$ and the triple- α reaction. The yield of a species is the its abundance in the ejected material minus the initial abundance integrated over the mass loss.

of the O-rich to C-rich transitions needs to be known. C-rich giants are the brightest infrared population in extra-galactic systems. Finally, the envelope enrichment of AGB stars with the s-process elements is intimately related to the dredge-up properties of the models.

Recently, it has been shown that uncertainties in nuclear reaction rates propagate in a significant way into the dredge-up and thereby yield predictions. Herwig & Austin (2004) calculated an extensive grid of $2 M_{\odot}$, $Z = 0.01$ tracks for combinations of rates for the ${}^{14}\text{N}(\text{p}, \gamma){}^{14}\text{O}$, the triple- α and the ${}^{12}\text{C}(\alpha, \gamma){}^{16}\text{O}$ rate within the errors given in the NACRE compilation (Angulo et al., 1999). The main result was that dredge-up and C yields are larger for lower ${}^{14}\text{N}(\text{p}, \gamma)$ rate and for larger triple- α rate. The ${}^{12}\text{C}(\alpha, \gamma)$ rate plays a less important role. It was also found that nuclear physics work since the 1999 NACRE compilation require a downward revision of the ${}^{14}\text{N}(p, \gamma)$ rate, by almost a factor of 2. Fig. 8 shows the revised range for this rate and the yields from the calculations assuming the uncertainty range of the nuclear reaction rates.

9 Conclusions

Extremely metal-poor stars are an emerging field of astrophysical and astronomical research, pushing the limits of observations, and theory and numerical simulation. Potentially, much can be learned about challenging questions of astrophysics. How do galaxies like our Milky Way form? How did the first stars and their cosmological environment form and evolve? Some exciting clues about the evolution of stars come from the smallest astrophysical bodies, pre-solar stardust extracted from primitive meteorites. Thus stellar evolution and nucleosynthesis connects nearby phenomena of planetary system formation with star formation and evolution in the earliest time of the universe as recorded in the element distribution patterns of the most metal-poor stars.

In the future the quantity and quality of spectroscopic data of stars, in particular the valuable most metal-poor stars, will increase dramatically, due to multi-object spectroscopy and large spectroscopic surveys. It is already becoming clear that this data can be put to full use only with qualitatively and quantitatively improved simulations of nuclear production in stars, including low and intermediate mass and massive stars.

Acknowledgements

I would like to thank D. Schoenberner for nominating me for the Ludwig-Biermann award, and for directing my interest to stellar evolution and nucleosynthesis as my *Doktorvater*. I am very grateful to N. Langer and D. VandenBerg for their continuing support. I would also like to thank my colleagues at the Theoretical Astrophysics group (T-6) at Los Alamos National Laboratory, in particular C. Fryer, A. Heger, and F. Timmes, as well as R. Reifarth at LANL-3, who contribute to a very stimulating atmosphere. Finally, I would like to thank A. Font and B. O'Shea for stimulating discussions, that have contributed to some views expressed in this article. This work was funded under the auspices of the U.S. Dept. of Energy, and supported by its contract W-7405-ENG-36 to Los Alamos National Laboratory.

References

Abel, T., Bryan, G. L., & Norman, M. L. 2002, Science, 295, 93

Angulo, C., Arnould, M., & Rayet, M. et al. 1999, Nucl. Phys., A 656, 3,
NACRE compilation

Aoki, W., Ando, H., Honda, S., Iye, M., Izumiura, H., Kajino, T., Kambe,
E., Kawanomono, S., Noguchi, K., Okita, K., Sadakane, K., Sato, B.,
Shelton, I., Takada-Hidai, M., Takeda, Y., Watanabe, E., & Yoshida, M.
2002, PASJ, 54, 427

Aoki, W., Ryan, S. G., Norris, J. E., Beers, T. C., Ando, H., Iwamoto, N.,
Kajino, T., Mathews, G. J., & Fujimoto, M. Y. 2001, ApJ, 561, 346

Arlandini, C., Käppeler, F., Wissak, K., Gallino, R., Lugaro, M., Busso, M., & Straniero, O. 1999, ApJ, 525, 886

Asplund, M., Lambert, D. L., Kipper, T., Pollacco, D., & Shetrone, M. D. 1999, A&A, 343, 507

Barbuy, B., Cayrel, R., Spite, M., Beers, T. C., Spite, F., Nordstroem, B., & Nissen, P. E. 1997, A&A, 317, L63

Beer, H., Voss, F., & Winters, R. R. 1992, ApJS, 80, 403

Beers, T. C. & Christlieb, N. 2005, ARAA, 43, in press

Beers, T. C., Preston, G. W., & Shectman, S. A. 1992, AJ, 103, 1987

Bessell, M. S., Christlieb, N., & Gustafsson, B. 2004, ApJ Lett., 612, L61

Bland-Hawthorn, J. & Freeman, K. 2000, Science, 287, 79

Böhm-Vitense, E. 1958, Z. Astrophys., 46, 108

Boothroyd, A. I. & Sackmann, I.-J. 1988, ApJ, 328, 671

Boothroyd, A. I., Sackmann, I.-J., & Ahern, S. C. 1993, ApJ, 416, 762

Busso, M., Gallino, R., Lambert, D. L., Travaglio, C., & Smith, V. V. 2001, ApJ, 557, 802

Busso, M., Gallino, R., & Wasserburg, G. J. 1999, ARA&A, 37, 239

Centurión, M., Molaro, P., Vladilo, G., Péroux, C., Levshakov, S. A., & D'Odorico, V. 2003, A&A, 403, 55

Chieffi, A., Dominguez, I., Limongi, M., & Straniero, O. 2001, ApJ, 554, 1159

Christlieb, N., Bessel, M. S., Beers, T. C., Gustafsson, B., Korn, A., Barklem, P. S., Karlsson, T., Mizuno-Wiedner, M., & Rossi, S. 2002, Nature, 419

Christlieb, N., Green, P. J., Wisotzki, L., & Reimers, D. 2001, A&A, 375, 366

Christlieb, N., Gustafsson, B., Korn, A. J., Barklem, P. S., Beers, T. C., Bessell, M. S., Karlsson, T., & Mizuno-Wiedner, M. 2004, ApJ, 603, 708

Denissenkov, P. A. & Tout, C. A. 2003, MNRAS, 340, 722

Denissenkov, P. A. & Vandenberg, D. A. 2003, ApJ, 593, 509

Duerbeck, H. W., Liller, W., Sterken, C., Benetti, S., van Genderen, A. M., Arts, J., Kurk, J. D., Janson, M., Voskes, T., Brogt, E., Arentoft, T., van der Meer, A., & Dijkstra, R. 2000, AJ, 119, 2360

Eck, S. van, Goriely, S., Jorissen, A. & Plez, B. 2003, A&A, 404, 291

Freeman, K. & Bland-Hawthorn, J. 2002, ARA&A, 40, 487

Fryer, C., Benz, W., Herant, M., & Colgate, S. A. 1999, ApJ, 516, 892

Fujimoto, M. Y., Ikeda, Y., & Iben, I., J. 2000, ApJ Lett., 529, L25

Gallino, R., Arlandini, C., Busso, M., Lugardo, M., Travaglio, C., Straniero, O., Chieffi, A., & Limongi, M. 1998, ApJ, 497, 388

Goriely, S. & Siess, L. 2001, A&A, 378, L25

—. 2004, A&A, 421, L25

Hajduk, M., Zijlstra, A. A., Herwig, F., & et al. 2005, Science, in press

Hamann, W.-R., Gräfener, G., & Koesterke, L. 2003, in Planetary Nebulae. Their Evolution and Role in the Universe, ed. M. D. et al., PASP Conf. Ser., IAU Symp 209, 203

Heber, U., Napiwotzki, R., & Reid, I. N. 1997, A&A, 323, 819

Heger, A., Langer, N., & Woosley, S. E. 2000, ApJ, 528, 368

Heger, A. & Woosley, S. E. 2002, ApJ, 567, 532

Herwig, F. 2000, A&A, 360, 952

—. 2001, ApJ Lett., 554, L71

—. 2003, in CNO in the Universe, ASP Conf. Ser. astro-ph/0212366

—. 2004a, ApJ, 605, 425

—. 2004b, ApJS, 155, 651

Herwig, F. 2005, ARAA, 43, in press

Herwig, F. & Austin, S. M. 2004, ApJ Lett., 613, L73

Herwig, F., Blöcker, T., Langer, N., & Driebe, T. 1999, A&A, 349, L5

Herwig, F., Blöcker, T., Schönberner, D., & El Eid, M. F. 1997, A&A, 324, L81

Herwig, F., Johnson, J., Beers, T. C., & Christlieb, N. 2004, BAAS 205

Herwig, F. & Langer, N. 2001, Nucl. Phys. A, 688, 221, astro-ph/0010120

Herwig, F., Langer, N., & Lugardo, M. 2003a, ApJ, 593, 1056

Herwig, F., Lugardo, M., & Werner, K. 2003b, in Planetary Nebulae. Their Evolution and Role in the Universe, ed. M. D. et al., PASP Conf. Ser., IAU Symp 209, astro-ph/0202143

Iben, Jr., I., Kaler, J. B., Truran, J. W., & Renzini, A. 1983, ApJ, 264, 605

Iwamoto, N., Kajino, T., Mathews, G. J., Fujimoto, M. Y., & Aoki, W. 2004, ApJ, 602, 378

Johnson, J., Herwig, F., Beers, T. C., & Christlieb, N. 2005, AJ, in prep.

Kawaler, S. D. 2003, in Stellar Rotation, ed. A. Maeder & P. Eenens, IAU Symp. 215, astro-ph/0301539

Koester, D., Dreizler, S., Weidemann, V., & Allard, N. F. 1998, A&A, 338, 612

Koesterke, L. 2001, Ap&SS, 275, 41

Laird, J. B. 1985, ApJ, 289, 556

Langer, N., Heger, A., Wellstein, S., & Herwig, F. 1999, A&A, 346, L37

Lucatello, S., Gratton, R., Cohen, J. G., Beers, T. C., Christlieb, N., Carretta, E., & Ramirez, S. 2003, AJ, 125, 875

Lucatello, S., Tsangarides, S., Beers, T. C., Carretta, E., Gratton, R. G., & Ryan, S. G. 2004, ArXiv Astrophysics e-prints, apJ, in press.

Lugardo, M., Davis, A. M., Gallino, R., Pellin, M. J., Straniero, O., & Käppeler, F. 2003a, ApJ, 593, 486

Lugardo, M., Herwig, F., Lattanzio, J. C., Gallino, R., & Straniero, O. 2003b, ApJ, 586, 1305

Lugardo, M., Ugalde, C., Karakas, A. I., Görres, J., Wiescher, M., Lattanzio, J. C., & Cannon, R. C. 2004, ApJ, 615, 934

Meynet, G. & Maeder, A. 2002, A&A, 390, 561

Miksa, S., Deetjen, J. L., Dreizler, S., Kruk, J. W., Rauch, T., & Werner, K. 2002, A&A, 389, 953

Nicolussi, G. K., Pellin, M. J., Lewis, R. S., Davis, A. M., Clayton, R. N., & Amari, S. 1998, Phys. Rev. Lett., 81, 3583

Nollett, K. M., Busso, M., & Wasserburg, G. J. 2003, ApJ, 582, 1036

Nomoto, K. 1984, ApJ, 277, 791

O’Shea, B., Abel, T., Norman, M. L., & Whalen, D. 2005, in prep.

Pettini, M., Ellison, S. L., Steidel, C. C., & Bowen, D. V. 1999, ApJ, 510, 576

Preston, G. W. & Sneden, C. 2001, AJ, 122, 1545

Prochaska, J. X., Henry, R. B. C., O’Meara, J. M., Tytler, D., Wolfe, A. M., Kirkman, D., Lubin, D., & Suzuki, N. 2002, PASP, 114, 933

Qian, Y.-Z. & Wasserburg, G. J. 2003, ApJ, 588, 1099

Robertson, B., Bullock, J. S., Font, A. S., Johnston, K. V., & Hernquist, L. 2005, ArXiv Astrophysics e-prints

Siess, L., Goriely, S., & Langer, N. 2004, A&A, 415, 1089

Siess, L., Livio, M., & Lattanzio, J. 2002, ApJ, 570, 329

Sivarani, T., Bonifacio, P., Molaro, P., Cayrel, R., Spite, M., Spite, F., Plez, B., Andersen, J., Barbuy, B., Beers, T. C., Depagne, E., Hill, V., François, P., Nordström, B., & Primas, F. 2004, A&A, 413, 1073

Suda, T., Aikawa, M., Machida, M. N., Fujimoto, M. Y., & Iben, I. J. 2004, ApJ, 611, 476

Umeda, H. & Nomoto, K. 2003, Nature, 422, 871

Van Winckel, H. & Reyniers, M. 2000, A&A, 354, 135

Venn, K. A., Irwin, M., Shetrone, M. D., Tout, C. A., Hill, V., & Tolstoy, E. 2004, AJ, 128, 1177

Weiss, A., Schlattl, H., Salaris, M., & Cassisi, S. 2004, A&A, 422, 217

Werner, K. 2001, Ap&SS, 275, 27

Werner, K., Rauch, T., & Kruk, J. W. 2005, A&A, astro-ph/0410690

Werner, K., Rauch, T., Reiff, E., Kruk, J. W., & Napiwotzki, R. 2004, A&A, 427, 685

Woosley, S. E. & Weaver, T. A. 1995, APJS, 101, 181

Young, P., Meakin, C., Fryer, C. L., & Arnett, D. 2005, ApJ, in prep.